

Layered aluminophosphates II.† Crystal structure and thermal behaviour of the layered aluminophosphate UiO-15 and its high temperature variants

Kjell Ove Kongshaug, Helmer Fjellvåg* and Karl Petter Lillerud

Department of Chemistry, University of Oslo, P.O. Box 1033 Blindern, N-0315 Oslo, Norway.

E-mail: helmer.fjellvag@kjemi.uio.no

Received 22nd February 1999, Accepted 30th March 1999

The synthesis and crystal structure of a novel layered aluminophosphate and its two high temperature variants are described. All three structures were solved from powder X-ray diffraction data. The as-synthesized material (UiO-15-as), with composition $[\text{NH}_3(\text{CH}_2)_2\text{NH}_3]^{2+}[\text{Al}_2(\text{OH})_2(\text{PO}_4)_2(\text{H}_2\text{O})]^{2-} \cdot \text{H}_2\text{O}$, crystallizes in the space group $P\bar{1}$ with $a = 10.37490(13)$, $b = 6.60775(8)$, $c = 9.90937(11)$ Å, $\alpha = 90.762(1)$, $\beta = 115.265(1)$ and $\gamma = 90.162(1)^\circ$. In the aluminophosphate layers the five- and six-coordinated aluminium polyhedra form infinite chains along [010] that are crosslinked by phosphate groups. These layers are held together by a complex hydrogen bonding scheme involving the terminal oxygen atoms of the phosphate groups and the nitrogens of the ethylenediammonium ions. A high temperature variant exists around 125 °C (UiO-15-125). This compound, with composition $[\text{NH}_3(\text{CH}_2)_2\text{NH}_3]^{2+}[\text{Al}_2(\text{OH})_2(\text{PO}_4)_2]^{2-}$, crystallizes in the monoclinic space group $P2_1/c$ with $a = 10.28899(23)$, $b = 6.75080(13)$, $c = 9.62527(20)$ Å and $\beta = 116.124(1)^\circ$. The transformation to UiO-15-125 involves removal of an interlamellar water molecule and another water molecule which is coordinated to aluminium. The infinite chains of aluminium polyhedra along [010] and the hydrogen bonding scheme of UiO-15-as is maintained in UiO-15-125. Another high temperature variant exists around 225 °C (UiO-15-225). This compound, with composition $[\text{NH}_3(\text{CH}_2)_2\text{NH}_3]^{2+}[\text{Al}_2\text{O}(\text{PO}_4)_2]^{2-}$, crystallizes in the monoclinic space group $P2_1/c$ with $a = 9.42781(37)$, $b = 6.91370(19)$, $c = 9.40823(27)$ Å and $\beta = 113.002(1)^\circ$. The transformation to UiO-15-225 involves the release of a water molecule from UiO-15-125 and the formation of tetrahedral Al–O–Al bonding. UiO-15-225 is therefore the first compound among the aluminophosphates violating Loewensteins rule.

Introduction

The search for new microporous compounds in the aluminophosphate system may at the same time lead to the discovery of new layered aluminophosphates. Known compounds of the latter type are composed of anionic 2D-aluminophosphate layers separated by protonated amine (or metallo-organic) cations where typically a complex hydrogen bonding scheme to the anionic layers is responsible for the 3D-integrity of the structure. The anionic aluminophosphate layers show a range of stoichiometries with P:Al molar ratios of 1:1,¹ 5:4,² 4:3,^{3–15} 3:2,^{16–19} and 2:1.^{14,20–22}

Structural transformations at elevated temperatures are well-known phenomena among the open-framework aluminophosphates. Examples include $\text{AlPO}_4\text{-21}/\text{AlPO}_4\text{-25}$,²³ $\text{AlPO}_4\text{-H}_3/\text{AlPO}_4\text{-C}/\text{AlPO}_4\text{-D}$ ²⁴ and $\text{VPI-5}/\text{AlPO}_4\text{-8}$.²⁵ There have been few studies on the thermal behaviour of layered aluminophosphates; most reports concentrate on the crystal structures of the as-synthesized materials. The importance of thermal studies on such materials is illustrated by the recent work of Oliver *et al.* which has revealed the existence of a high temperature aluminophosphate chain to layer transformation.¹⁸ On the basis of their study they have proposed a model for the formation of aluminophosphates in which two- and three-dimensional structures are formed upon hydrolysis and condensation of an initial chain structure.²⁶

This paper reports the hydrothermal synthesis of a novel layered aluminophosphate with a molar P:Al ratio of 1:1. The as-synthesized room temperature variant is denoted UiO-15-as. The thermal behaviour of this water and template containing material has been investigated. On dehydration, two high temperature variants appear, one around 125 °C

(UiO-15-125) and a second around 225 °C (UiO-15-225). Their crystal structures have been solved from powder X-ray diffraction data. Special emphasis is put on describing temperature induced changes in Al-coordination and in Al-polyhedra connectivity.

Experimental

UiO-15-as was prepared by hydrothermal synthesis under autogeneous pressure. The reactants were hydrated aluminium hydroxide (55% Al_2O_3 , 45% H_2O , Aldrich), phosphoric acid (85%, Merck), ethylenediamine (97%, Fluka) and water. The molar composition of the starting gel was 1 Al_2O_3 :3.5 H_3PO_4 :3 ethylenediamine:40 H_2O . The crystallization took place at 150 °C in a Teflon-lined autoclave over 12 h. The obtained polycrystalline product was filtered off, washed with water and dried in air at 80 °C overnight.

The high temperature variants of UiO-15 were obtained by calcination at 125 and 225 °C in a nitrogen atmosphere for 10 h, giving UiO-15-125 and UiO-15-225 respectively.

The Al and P contents in UiO-15-as were determined from energy dispersive X-ray analysis (EDX) with a Philips SEM. They corresponded to a molar P:Al ratio of 97:100. Thermal analyses were performed with a Rheometric Scientific STA 1500. The sample was heated in a nitrogen gas flow at a rate of 5 K min^{-1} .

High temperature powder X-ray diffraction data (HT-PXRD) were collected using a Bühler furnace on a Siemens D500 instrument in Bragg–Brentano geometry with $\text{Cu-K}\alpha$ radiation. The sample was smeared on a platinum filament and data were collected at 25 °C and between 100 and 400 °C in steps of $\Delta T = 25$ °C.

High resolution powder X-ray diffraction data were collected in transmission mode at 25 °C with a Siemens D5000

†For Part I, see ref. 1.

diffractometer with monochromated Cu-K α_1 radiation ($\lambda = 1.540598 \text{ \AA}$) selected with an incident-beam germanium monochromator. The detector was a Brown PSD. The powder samples were loaded into 0.5 mm diameter borosilicate capillaries. The diffraction patterns were collected over the 2θ range $8-90^\circ$. Total counting time was around 36 h.

Characterization and structure determination

Structure determination of UiO-15-as

The powder diffraction pattern was autoindexed with the TREOR-90 program²⁷ on the basis of the first 20 Bragg reflections. The best solution (FOM = 70) indicated a triclinic unit cell with dimensions $a = 10.368$, $b = 6.605$, $c = 9.907 \text{ \AA}$, $\alpha = 90.77$, $\beta = 115.31$ and $\gamma = 90.15^\circ$. Integrated intensities were extracted from the pattern assuming space group $P\bar{1}$ by means of the FULLPROF program.²⁸ This program applies the Le Bail method²⁹ for extraction of intensities. The intensities were introduced into SIRPOW.92,³⁰ a direct method program specially designed for structure solution from powder data. By means of the Cerius² graphical software³¹ all Al, P, O, C and N atomic positions in the structure were located from the E -map with the highest figure-of-merit. These atomic positions were thereafter used as starting models for Rietveld refinements using the GSAS program.³² After initial refinement of zero point, scale, background and unit-cell parameters, atomic coordinates were refined with soft constraints being introduced: $d(\text{Al-O}) = 1.85(\pm 2)$, $d(\text{P-O}) = 1.53(\pm 2)$, $d(\text{Al-P}) = 3.15(\pm 5)$ (for angle restraints), $d(\text{C-N}) = 1.48(\pm 2)$ and $d(\text{C-C}) = 1.52(\pm 2) \text{ \AA}$. At this stage successive difference Fourier maps revealed the positions of two additional water molecules. The refinement progressed well with these two positions added to the model. In the next stage of the refinement common isotropic displacement parameters were adopted for phosphorus, aluminium, oxygen and template nitrogen and carbon. However, this resulted in a negative value for the displacement parameter of the template. Hydrogen positions were therefore added with soft constraints $d(\text{N-H}) = 1.03(\pm 1)$ and $d(\text{C-H}) = 1.08(\pm 1) \text{ \AA}$ and given a constant common isotropic displacement parameter of 0.05 \AA^2 . Hydrogen atoms were also added to the two water oxygens along with soft constraints $d(\text{O-H}) = 1.03(\pm 1) \text{ \AA}$ and the same common displacement parameter of 0.05 \AA^2 . This resulted in a marked improvement in the displacement parameter refinement and in the overall refinement. In the last stage of the refinement the weight of the soft constraints could be relaxed, and the refinement involving 146 parameters converged to satisfactory residual factors $R_F^2 = 0.029$ and $R_{wp} = 0.029$.

Experimental conditions and details of the Rietveld refinement are reported in Table 1. Fig. 1 shows the observed, calculated and difference diffraction profiles from the Rietveld analysis. Atomic coordinates and isotropic displacement parameters are given in Table 2 and selected bond distances and angles are presented in Table 3.

Thermal behaviour of UiO-15

A three-dimensional representation of the progressive change in the high temperature powder diffraction patterns which occur over the temperature range $25-400^\circ\text{C}$ is shown in Fig. 2. The patterns clearly reveal that the decomposition of UiO-15 proceeds through three stages. The same three stages correspond to three rather distinct weight losses as evident from the TGA curve (Fig. 3). The first weight loss of approximately 10% corresponds to the release of two water molecules (calculated 9.58%). The same dehydration process can be identified from Fig. 2 where the anhydrous phase has emerged fully at 125°C (UiO-15-125) with a diffraction pattern distinctly different from that of the as-synthesized variant. The next

Table 1 Experimental conditions and relevant data for the Rietveld refinements of UiO-15-as, UiO-15-125 and UiO-15-225

	UiO-15-as	UiO-15-125	UiO-15-225
Pattern range $2\theta/^\circ$	8–90	8–90	8–90
Step size $\Delta 2\theta/^\circ$	0.015552	0.015552	0.015552
Wavelength/ \AA	1.540598	1.540598	1.540598
Space group	$P\bar{1}$	$P2_1/c$	$P2_1/c$
$a/\text{\AA}$	10.37490(13)	10.28899(23)	9.42781(37)
$b/\text{\AA}$	6.60775(8)	6.75080(13)	6.91370(19)
$c/\text{\AA}$	9.90937(11)	9.62527(20)	9.40823(27)
$\alpha/^\circ$	90.762(1)	90	90
$\beta/^\circ$	115.265(1)	116.124(1)	113.002(1)
$\gamma/^\circ$	90.162(1)	90	90
Z	2	4	4
$V/\text{\AA}^3$	614.272(13)	600.266(23)	564.482(35)
No. observations	5264	5258	5258
No. reflections	1063	542	517
No. refined params.	146	84	81
R_{wp}	0.0286	0.0344	0.0380
R_F^2	0.0289	0.0450	0.0492

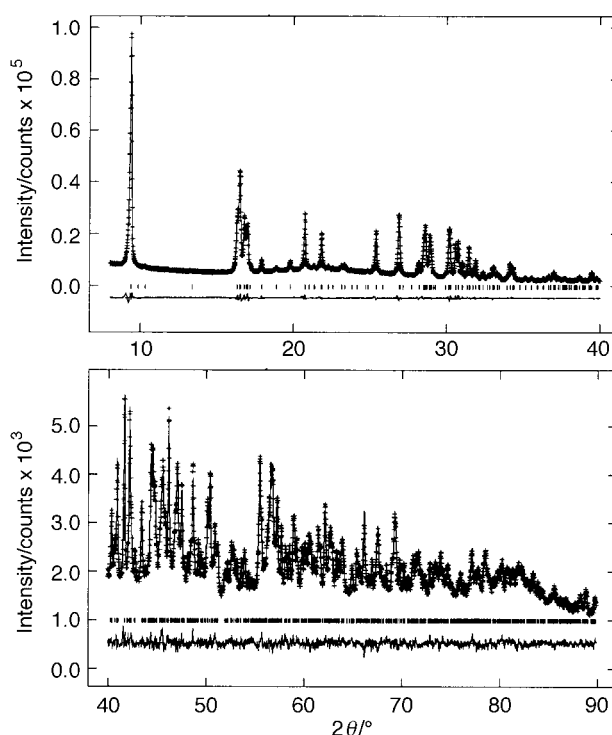


Fig. 1 Observed, calculated and difference diffraction profiles for UiO-15-as.

phase transformation is completed around 225°C (UiO-15-225) and is accompanied by another weight loss (Fig. 3). The total weight loss of 14.8% at this stage is consistent with the release of a third water molecule (calculated 14.37%). Again this transformation results in a diffraction pattern distinctly different from those of the other two phases (Fig. 2). Finally, on further heating UiO-15-225 transforms into an amorphous phase when the ethylenediammonium ions leave the material at around 300°C . For the amorphous phase, the observed total weight loss is 30.68% (calculated 30.89%).

Structure determination of UiO-15-125

The first dehydration step of UiO-15-as is irreversible, and therefore high resolution powder X-ray diffraction data could be collected at 25°C for a sample of UiO-15-125 obtained by calcination at 125°C . Its diffraction pattern was indexed from the first 20 Bragg reflections with the program TREOR-90,²⁷ leading to a monoclinic unit cell: $a = 10.286$, $b = 6.75$, $c =$

Table 2 Atomic coordinates and isotropic displacement parameters for UiO-15-as derived from Rietveld refinement in space group $P\bar{1}$. Calculated standard deviation in parentheses

Atom	<i>x</i>	<i>y</i>	<i>z</i>	$U_{\text{iso}}/\text{\AA}^2$
P1	0.69788(32)	0.1078(5)	0.5136(4)	0.0237(9)
P2	0.71125(31)	0.4095(5)	0.03001(35)	0.0237(9)
Al1	0.5409(4)	0.1718(6)	0.7280(4)	0.0290(9)
Al2	0.5211(4)	0.3303(6)	0.2106(4)	0.0290(9)
O1	0.8566(7)	0.0736(10)	0.5884(6)	0.0189(7)
O2	0.6648(6)	0.2735(10)	0.3930(6)	0.0189(7)
O3	0.6121(6)	0.9093(9)	0.4471(6)	0.0189(7)
O4	0.6542(6)	0.2052(9)	0.6305(7)	0.0189(7)
O5	0.8676(6)	0.4503(9)	0.1241(6)	0.0189(7)
O6	0.3583(6)	0.6978(9)	0.8784(7)	0.0189(7)
O7	0.6934(6)	0.2576(10)	0.8956(7)	0.0189(7)
O8	0.3694(6)	0.3960(10)	0.0372(7)	0.0189(7)
O9 ^b	0.5426(6)	0.9411(10)	0.8296(6)	0.0189(7)
O10 ^b	0.4366(6)	0.3894(9)	0.7301(6)	0.0189(7)
OW1	0.6232(8)	0.6493(12)	0.6825(8)	0.033(3)
OW2	0.2230(7)	0.0864(12)	0.8002(8)	0.053(3)
N1	0.9762(8)	0.2524(11)	0.3985(8)	0.030(2)
N2	0.9672(9)	0.2310(11)	0.8826(9)	0.030(2)
C1	0.0533(10)	0.4214(15)	0.5028(12)	0.030(2)
C2	0.0467(11)	0.0977(15)	0.0096(12)	0.030(2)
H1	0.958(6)	0.161(7)	0.784(3)	0.05 ^a
H2	0.025(5)	0.362(5)	0.894(6)	0.05 ^a
H3	0.866(3)	0.253(9)	0.873(5)	0.05 ^a
H4	0.889(4)	0.210(8)	0.411(6)	0.05 ^a
H5	0.947(6)	0.309(6)	0.290(2)	0.05 ^a
H6	0.043(4)	0.132(5)	0.406(6)	0.05 ^a
H7	0.142(5)	0.465(10)	0.475(7)	0.05 ^a
H8	0.109(6)	0.335(10)	0.602(5)	0.05 ^a
H9	0.948(7)	0.807(10)	0.899(6)	0.05 ^a
H10	0.848(4)	0.909(12)	-0.013(8)	0.05 ^a
H11	0.692(6)	0.535(8)	0.680(8)	0.05 ^a
H12	0.645(8)	0.756(8)	0.617(7)	0.05 ^a
H13	0.319(5)	0.093(12)	0.786(8)	0.05 ^a
H14	0.273(7)	0.098(12)	0.918(2)	0.05 ^a

^aFixed. ^bProbably OH.

9.62 Å and $\beta = 116.12^\circ$ (FOM=76). A careful inspection of the powder pattern indicated extinguished reflections $0k0$ for $k=2n+1$ and $h0l$ and $00l$ for $l=2n+1$. This is consistent with space group $P2_1/c$. The unit cell dimensions are clearly related to those of UiO-15-as, and hence a starting model for the structure of UiO-15-125 could be built. By means of the InsightII software,³³ two water molecules and the template ethylenediammonium ions were removed from the structure of UiO-15-as, the unit cell was transformed from the triclinic to the monoclinic crystal system and the space group was changed from $P\bar{1}$ to $P2_1/c$. Bond distances and angles were thereafter optimized using the DLS program.³⁴

This starting model was transferred into the GSAS program for Rietveld refinements. Soft constraints were introduced: $d(\text{Al}-\text{O})=1.83(\pm 2)$, $d(\text{P}-\text{O})=1.53(\pm 2)$, $d(\text{Al}-\text{P})=3.15(\pm 5)$ Å (for angle restraints). Refinement of scale, background, zero point, lattice parameters and atomic positions for Al, P and O was followed by successive difference Fourier maps which located the template carbon and nitrogen atoms. Soft constraints were also introduced for these atoms: $d(\text{C}-\text{N})=1.48(\pm 2)$, $d(\text{C}-\text{C})=1.52(\pm 2)$ Å, and the C and N positions were refined. In the next stage of the refinement, isotropic displacement parameters were refined and common parameters were introduced for aluminium, phosphorus, oxygen and template carbon and nitrogen. As for UiO-15-as the refined displacement parameter for C and N was negative. Hydrogen positions were again introduced along with soft constraints $d(\text{N}-\text{H})=1.03(\pm 1)$ and $d(\text{C}-\text{H})=1.08(\pm 1)$ Å and given a constant common isotropic displacement parameter of 0.05 Å². The refinements converged to satisfactory residual factors $R_F^2=0.045$ and $R_{\text{wp}}=0.034$. The weight of the soft constraints was relaxed during the last cycles of the refinement, which

Table 3 Bond distances (Å) and selected bond angles (°) for UiO-15-as. Calculated standard deviations in parentheses

Distances		Angles	
P1-O1	1.509(6)	O1-P1-O2	109.1(4)
P1-O2	1.559(6)	O1-P1-O3	112.4(4)
P1-O3	1.555(6)	O1-P1-O4	107.7(4)
P1-O4	1.546(6)	O2-P1-O3	111.9(4)
		O2-P1-O4	104.2(4)
		O3-P1-O4	111.1(4)
P2-O5	1.507(6)	O5-P2-O6	111.2(4)
P2-O6	1.555(6)	O5-P2-O7	109.2(4)
P2-O7	1.603(6)	O5-P2-O8	111.7(3)
P2-O8	1.532(7)	O6-P2-O7	106.4(3)
		O6-P2-O8	110.0(4)
		O7-P2-O8	108.1(4)
Al1-O3	1.854(6)	O3-Al1-O4	91.6(3)
Al1-O4	1.827(6)	O3-Al1-O7	177.8(4)
Al1-O7	1.820(6)	O3-Al1-O9	95.0(3)
Al1-O9	1.834(7)	O3-Al1-O10	87.2(3)
Al1-O10	1.808(6)	O4-Al1-O7	86.6(3)
		O4-Al1-O9	122.6(4)
		O4-Al1-O10	115.4(3)
		O7-Al1-O9	86.0(3)
		O7-Al1-O10	92.5(3)
		O9-Al1-O10	121.8(3)
Al2-O2	1.831(6)	O2-Al2-O6	91.0(3)
Al2-O6	1.822(6)	O2-Al2-O8	175.1(4)
Al2-O8	1.826(6)	O2-Al2-O9	93.7(3)
Al2-O9	1.887(7)	O2-Al2-O10	85.8(3)
Al2-O10	1.927(7)	O2-Al2-OW1	88.4(3)
Al2-OW1	2.176(7)	O6-Al2-O8	93.6(3)
		O6-Al2-O9	93.2(4)
		O6-Al2-O10	97.3(3)
		O6-Al2-OW1	177.7(4)
		O8-Al2-O9	87.5(3)
		O8-Al2-O10	92.2(3)
		O8-Al2-OW1	87.0(3)
		O9-Al2-O10	169.5(4)
		O9-Al2-OW1	84.58(3)
		O10-Al2-OW1	84.9(3)
N1-C1	1.488(12)	N1-C1-C1	108.5(1)
N2-C2	1.479(13)	N2-C2-C2	107.7(1)
C1-C1	1.504(16)		
C2-C2	1.573(15)		

involved 84 parameters. For details of the refinements, see Table 1. The observed, calculated and difference diffraction profiles from the refinement are shown in Fig. 4. Final atomic coordinates and displacement parameters are presented in Table 4, with selected bond distances and angles in Table 5.

Structure determination of UiO-15-225

The second step in the dehydration of UiO-15-as via UiO-15-125 into UiO-15-225 is also irreversible. Hence, high resolution powder X-ray diffraction data could be collected at 25 °C for

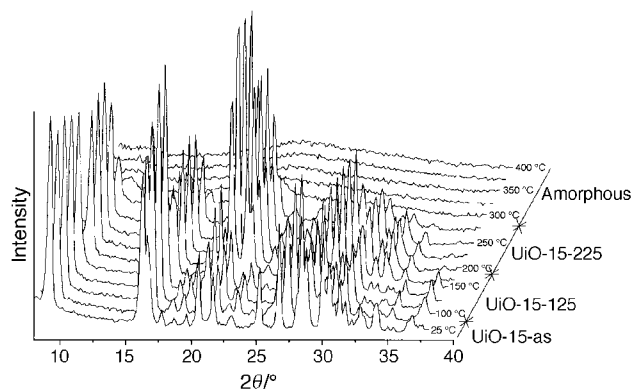


Fig. 2 3D-representation of high-temperature powder X-ray data for UiO-15.

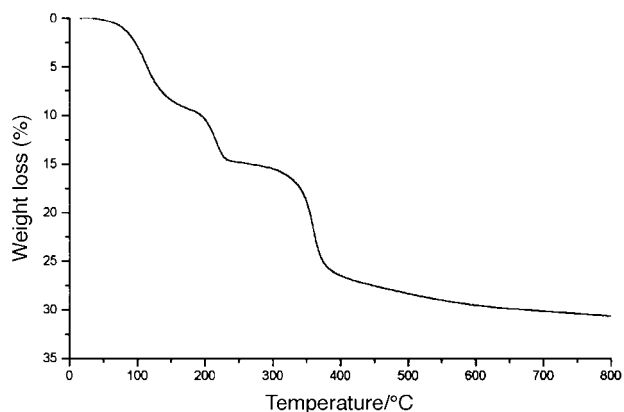


Fig. 3 TGA curve for UiO-15, heated in nitrogen at a rate of 5 K min⁻¹.

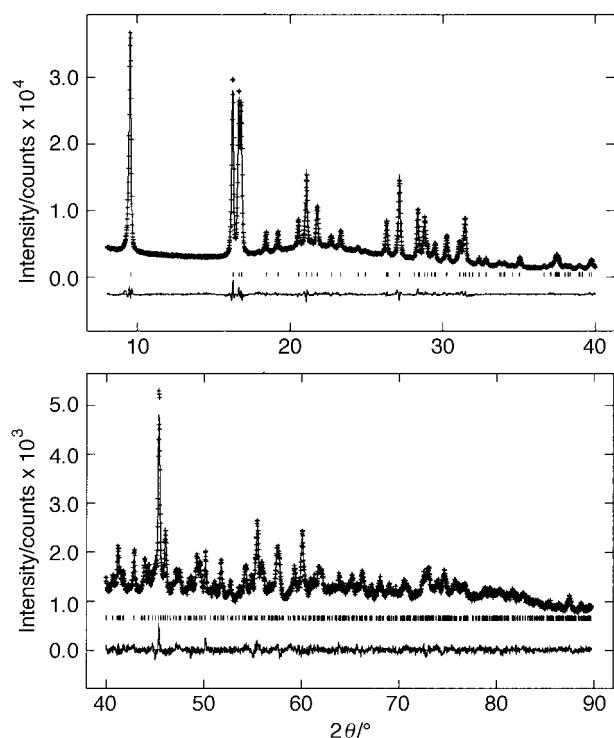


Fig. 4 Observed, calculated and difference diffraction profiles for UiO-15-125.

Table 4 Atomic coordinates and isotropic displacement parameters for UiO-15-125 derived from Rietveld refinement in space group $P2_1/c$. Calculated standard deviation in parentheses

Atom	x	y	z	$U_{iso}/\text{Å}^2$
P	0.70115(29)	0.4161(5)	0.03495(29)	0.027(1)
Al	0.53473(34)	0.1565(5)	0.7307(4)	0.030(1)
O1	0.8628(5)	0.0751(9)	0.5883(5)	0.021(1)
O2	0.3257(5)	0.6138(8)	0.8248(6)	0.021(1)
O3	0.6295(5)	0.8931(9)	0.4434(6)	0.021(1)
O4	0.6395(6)	0.2697(9)	0.4264(6)	0.021(1)
O5 ^b	0.4864(5)	0.4236(10)	0.6768(5)	0.021(1)
N	0.0275(7)	-0.2522(11)	0.5977(7)	0.031(2)
C	-0.0567(8)	-0.4210(14)	0.4991(10)	0.031(2)
H1	0.113(4)	-0.215(7)	0.579(5)	0.05 ^a
H2	0.057(5)	-0.291(6)	0.711(2)	0.05 ^a
H3	-0.049(4)	-0.140(5)	0.575(5)	0.05 ^a
H4	0.134(4)	0.372(6)	0.614(3)	0.05 ^a
H5	0.127(4)	0.457(7)	0.446(4)	0.05 ^a

^aFixed. ^bProbably OH.

Table 5 Bond distances (Å) and selected bond angles (°) for UiO-15-125. Calculated standard deviations in parentheses

Distances		Angles	
P-O1	1.511(5)	O1-P-O2	108.0(3)
P-O2	1.506(5)	O1-P-O3	109.7(4)
P-O3	1.552(6)	O1-P-O4	108.6(4)
P-O4	1.576(6)	O2-P-O3	113.0(4)
		O2-P-O4	108.0(4)
		O3-P-O4	109.4(3)
Al-O2	1.763(4)	O2-Al-O3	104.0(3)
Al-O3	1.811(4)	O2-Al-O4	99.9(3)
Al-O4	1.781(5)	O2-Al-O5	102.0(3)
Al-O5	1.881(6)	O2-Al-O5	106.8(3)
		O3-Al-O4	156.0(3)
		O3-Al-O5	84.1(3)
		O3-Al-O5	91.6(2)
		O4-Al-O5	89.3(2)
		O4-Al-O5	82.8(3)
		O5-Al-O5	150.1(2)
C-N	1.492(12)	N-C-C	106.9(8)
C-C	1.576(15)		

a UiO-15-225 sample obtained by calcination at 225 °C. The pattern was indexed with the DICVOL91 program,³⁵ and the best solution gave a monoclinic cell: $a=9.431$, $b=6.917$, $c=9.420$ Å and $\beta=112.97^\circ$ (FOM=33). The extinguished reflections $0k0$ ($k=2n+1$), $h0l$ and $00l$ ($l=2n+1$) suggested the space group $P2_1/c$. The crystal structure of UiO-15-225 was solved with the EXPO program³⁶ which integrates the Le Bail method based program EXTRA³⁷ for the extraction of intensities with SIRPOW.92.³⁰ EXPO ran several cycles using fragment information in the extraction process before a solution emerged where all Al, P, O, C and N atoms could be located from the peaks in the E -map by means of the Cerius² graphical software.³¹

The determined atomic positions were introduced into the GSAS program³² for Rietveld refinements. The refinement proceeded with variation of the scale, background, zero point and unit cell parameters. Atomic coordinates were subjected to soft constraints: $d(\text{Al-O})=1.75(\pm 2)$, $d(\text{P-O})=1.53(\pm 2)$, $d(\text{Al-P})=3.15(\pm 5)$, $d(\text{C-N})=1.48(\pm 2)$, $d(\text{C-C})=1.52(\pm 2)$ Å. Isotropic displacement parameters were refined and common parameters were adopted for oxygen and template carbon and nitrogen atoms. Coordinates for hydrogen positions were again subjected to soft constraints $d(\text{N-H})=1.03(\pm 1)$ and $d(\text{C-H})=1.08(\pm 1)$ Å with non-refinable isotropic displacement parameters of 0.05 Å^2 . This gave satisfactory residual factors $R_F^2=0.049$ and $R_{wp}=0.038$ with a total of 81 refinable parameters. The weight of the soft constraints could not be removed without unrealistic bond distances emerging in the structure, and was therefore kept at a value of 750 in the last cycles of the refinement. For further details, see Table 1. Atomic coordinates and isotropic displacement parameters are given in Table 6, and selected bond distances and angles in Table 7. The observed, calculated and difference diffraction profiles from the refinement are shown in Fig. 5.

Crystal structures and phase transformations

Crystal structure of UiO-15-as

The crystal structure of UiO-15-as, $[\text{NH}_3(\text{CH}_2)_2\text{NH}_3]^{2+}[\text{Al}_2(\text{OH})_2(\text{PO}_4)_2(\text{H}_2\text{O})]^{2-}\cdot\text{H}_2\text{O}$, is of a 2D-nature as shown in Fig. 6(a). Layers of anionic aluminophosphate are stacked along $[100]$ separated by ethylenediammonium ions and water molecules. In the aluminophosphate layers, aluminium is both five- and six-coordinated whereas phosphorus is four-coordinated. Both of the crystallographically distinct P tetrahedra possess three bridging oxygens with average bond lengths of $d(\text{P1-O})=1.553$ and $d(\text{P2-O})=1.563$ Å and one terminal oxygen each with bond lengths of $d(\text{P1-O1})=1.509$ and

Table 6 Atomic coordinates and isotropic displacement parameters for UiO-15-225 derived from Rietveld refinement in space group $P2_1/c$. Calculated standard deviations in parentheses

Atom	x	y	z	$U_{iso}/\text{\AA}^2$
P	0.3061(4)	0.0510(6)	0.8023(4)	0.039(2)
Al	0.5186(5)	-0.2997(5)	0.9076(5)	0.030(2)
O1	0.1425(6)	0.0743(12)	0.7039(8)	0.025(1)
O2	0.3438(6)	-0.1732(8)	0.8220(8)	0.025(1)
O3	0.6530(7)	-0.1406(10)	1.0356(7)	0.025(1)
O4	0.4122(7)	0.1477(11)	0.7341(7)	0.025(1)
O5	0.5000	0.5000	0.0000	0.025(1)
N	-0.0230(10)	-0.2625(10)	0.5807(9)	0.050(3)
C	0.9388(7)	0.0729(12)	0.9509(12)	0.050(3)
H1	0.024(4)	-0.135(1)	0.563(7)	0.05 ^a
H2	-0.138(2)	-0.269(5)	0.508(4)	0.05 ^a
H3	0.013(6)	0.271(5)	0.306(2)	0.05 ^a
H4	-0.121(5)	0.378(4)	0.521(5)	0.05 ^a
H5	-0.145(5)	0.479(5)	0.343(2)	0.05 ^a

^aFixed.

Table 7 Bond distances (\AA) and selected bond angles ($^\circ$) for UiO-15-225. Calculated standard deviations in parentheses.

Distances		Angles	
P-O1	1.466(5)	O1-P-O2	108.3(5)
P-O2	1.585(4)	O1-P-O3	111.9(5)
P-O3	1.549(4)	O1-P-O4	112.6(4)
P-O4	1.536(5)	O2-P-O3	108.6(4)
		O2-P-O4	108.8(4)
		O3-P-O4	106.6(4)
Al-O2	1.758(5)	O2-Al-O3	107.4(3)
Al-O3	1.753(4)	O2-Al-O4	108.6(4)
Al-O4	1.737(4)	O2-Al-O5	112.2(3)
Al-O5	1.6805(30)	O3-Al-O4	105.7(4)
		O3-Al-O5	110.8(3)
N-C	1.482(5)	O4-Al-O5	111.8(4)
C-C	1.538(6)	N-C-C	106.8(7)

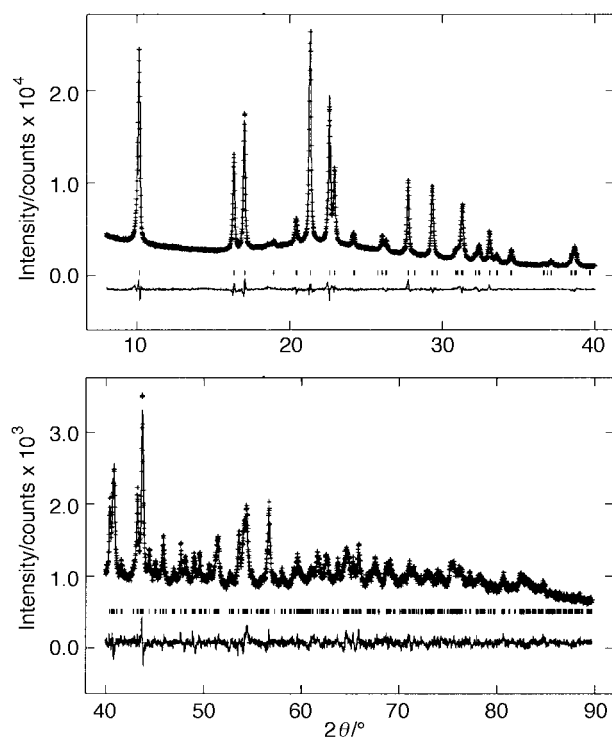


Fig. 5 Observed, calculated and difference diffraction profiles for UiO-15-225.

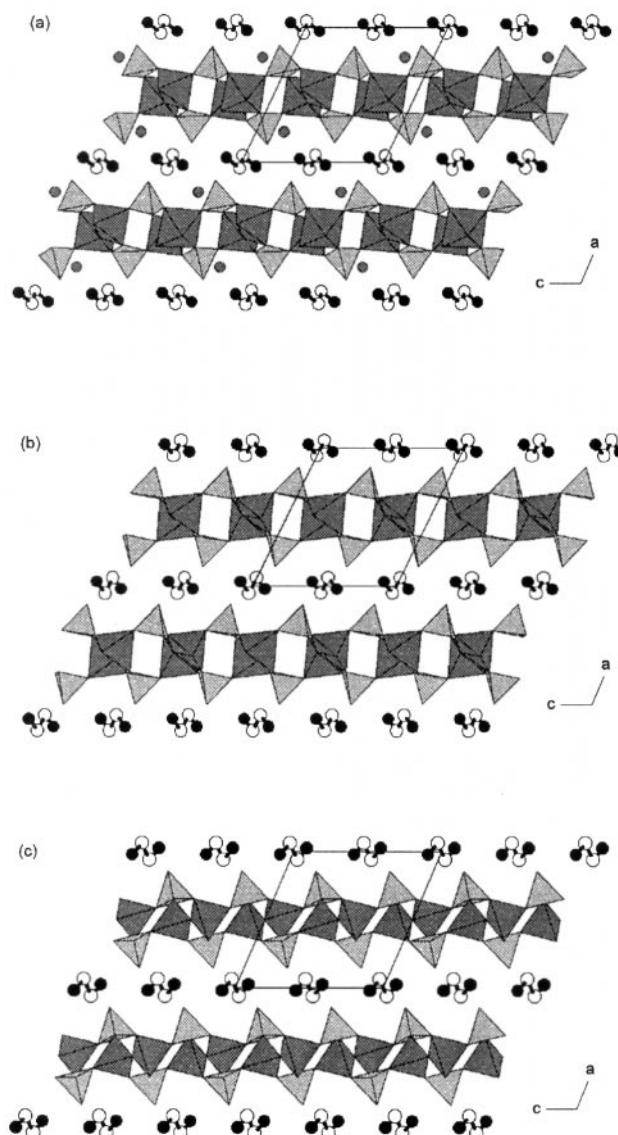


Fig. 6 Polyhedral representation of (a) UiO-15-as, (b) UiO-15-125 and (c) UiO-15-225. All structures seen along the [010]. Al polyhedra with darker shading, PO_4 tetrahedra with lighter shading, C atoms with open circles, water oxygens with shaded circles, N atoms with filled circles.

$d(\text{P2-O5}) = 1.507 \text{ \AA}$. The five-coordinated aluminium (Al1) forms a slightly distorted trigonal bipyramid with three bridging oxygens (O3, O4 and O7) to phosphorus with bond distances between 1.820 and 1.854 \AA and two oxygens (O9 and O10) connected to neighbouring aluminium octahedra at distances of $d(\text{Al1-O9}) = 1.834$ and $d(\text{Al1-O10}) = 1.808 \text{ \AA}$. Bond valence calculations³⁸ suggest that protons should be attached to the latter two oxygen atoms turning them into bridging OH groups. The six-coordinated aluminium (Al2) in octahedral surroundings is coordinated by three bridging oxygens (O2, O6 and O8) to phosphorus at bond distances between 1.822 and 1.831 \AA . Furthermore, there are bridging OH groups (O9 and O10) to neighboring aluminium trigonal bipyramids at distances $d(\text{Al2-O9}) = 1.887$ and $d(\text{Al2-O10}) = 1.927 \text{ \AA}$. The octahedron is completed by a sixth oxygen associated with a water molecule at a distance of $d(\text{Al2-OW1}) = 2.176 \text{ \AA}$. A similarly distorted aluminium octahedron is present in AlPO_4 ^{15,39} where the aluminium-water bond distance is 2.201 \AA . The OW1 water molecule participates in intralayer hydrogen bonding to O3 [$d(\text{O}\cdots\text{O}) = 2.88 \text{ \AA}$] and O4 [$d(\text{O}\cdots\text{O}) = 3.01 \text{ \AA}$]. Also the interlamellar water molecule

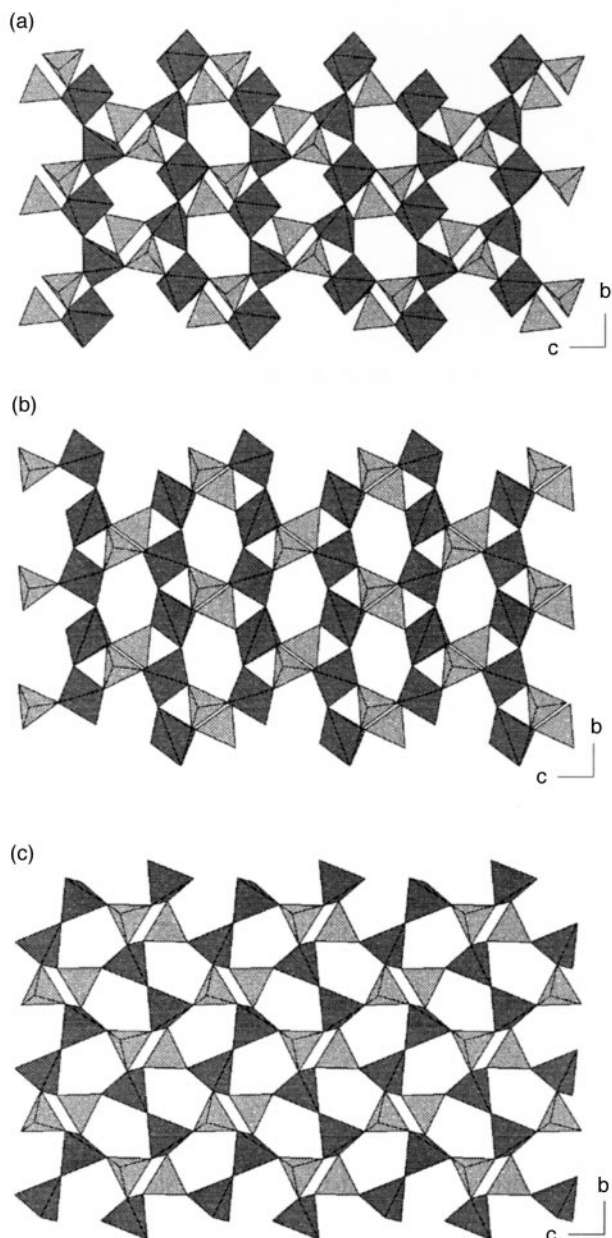


Fig. 7 Polyhedral representation of (a) UiO-15-as, (b) UiO-15-125 and (c) UiO-15-225. All structures seen along [100]. Al polyhedra with darker shading, PO₄ tetrahedra with lighter shading.

(OW2) participates in intralayer hydrogen bonding to O6 [$d(\text{O}\cdots\text{O})=2.89 \text{ \AA}$] and O8 [$d(\text{O}\cdots\text{O})=2.97 \text{ \AA}$].

The aluminium polyhedra form infinite chains along [010] [Fig. 7(a)] that are crosslinked by phosphate groups. The resulting layer structure is closely related to those which exist in a fluoroaluminophosphate,⁴⁰ in an aluminium methylphosphonate⁴¹ and in a vanadium hydrogenphosphate.⁴² In all these cases the chains are just made of octahedra whereas the chains in UiO-15-as consist of aluminium octahedra and trigonal bipyramids. The layers can alternatively be considered in terms of three-, four- and six-membered rings as illustrated in Fig. 8(a).

The aluminophosphate layers are held together by a complex hydrogen bonding scheme in which the terminal phosphonyl oxygen atoms (O1 and O5) and nitrogen atoms of the ethylenediammonium ions participate (Table 8). The ethylenediammonium ions are oriented parallel to the inorganic layers. One of the two nitrogen atoms of the template ion participates in two hydrogen bonds to the layer above and in one to that below, whereas the second nitrogen participates in two hydro-

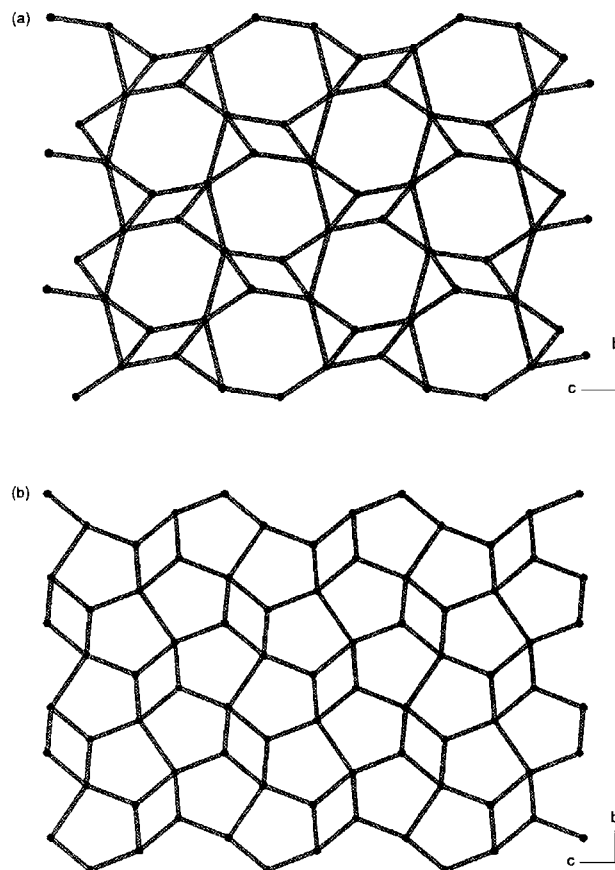


Fig. 8 2D layer of (a) UiO-15-as/125 seen along [100], showing the presence of three-, four- and six-membered rings, and (b) UiO-15-225 seen along [100], showing the presence of four- and five-membered rings.

Table 8 Probable hydrogen bond lengths in UiO-15-as

Hydrogen bond	Distance/Å
N1...O1	2.92
N1...O1	2.74
N1...O5	2.80
N2...O1	2.82
N2...O5	2.73
N2...O7	2.90

gen bonds to the layer below and one to that above (Fig. 9). The terminal phosphonyl oxygens are hydrogen bond acceptors. The diffraction data indicate that each O1 accepts three hydrogen bonds whereas each O5 accepts two hydrogen bonds. The last hydrogen bond connected to the nitrogen atoms is directed towards the bridging oxygen O7.

Crystal structure of UiO-15-125

UiO-15-125, $[\text{NH}_3(\text{CH}_2)_2\text{NH}_3]^{2+}[\text{Al}_2(\text{OH})_2(\text{PO}_4)_2]^{2-}$, is the anhydrous variant of UiO-15-as [Fig. 6(b)]. The transformation of UiO-15-as to UiO-15-125 involves removal of both the interlamellar water molecule and the water molecule bonded to the aluminium octahedra, see above. The unit cell symmetry changes from triclinic to monoclinic, but the cell dimensions are clearly related (Table 1). The symmetry change from $P\bar{1}$ to $P2_1/c$ implies single crystallographic sites for both Al and P. The coordination properties for the PO₄-tetrahedra remain as in UiO-15-as with three bridging oxygens (O2, O3 and O4) to aluminium with an average bond length of $d(\text{P}-\text{O})=1.545 \text{ \AA}$ (Table 5). The fourth oxygen of the tetrahedron is terminal, and is formally a double-bonded phosphonyl oxygen at a distance of $d(\text{P}-\text{O}1)=1.511 \text{ \AA}$. The

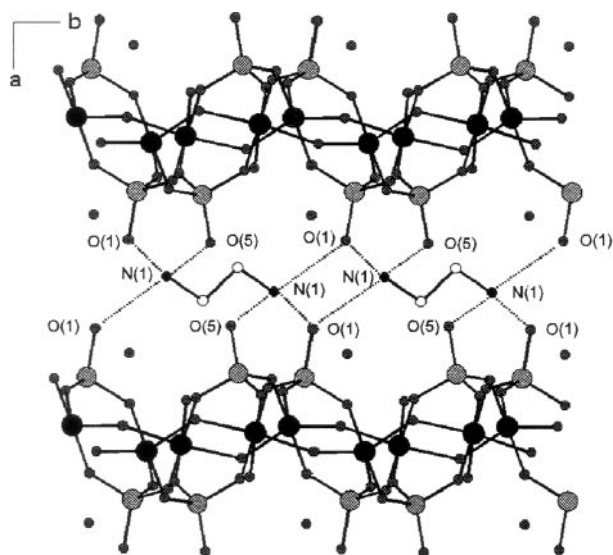


Fig. 9 UiO-15-as seen along [001] showing the hydrogen bonding scheme.

aluminium now becomes five-coordinated with three bridging oxygens to phosphorus [$d(\text{Al}-\text{O})$ between 1.763 and 1.811 Å] and with two bridging OH groups (O5 and O5'; as assigned from bond valence calculations) to neighbouring Al [$d(\text{Al}-\text{OH})=1.867$ and 1.881 Å].

There is only scarce information available on aluminophosphates containing solely five-coordinated aluminium: two layered aluminophosphates¹ and two MeAPO_5 ^{43,44} are known. The geometry of the aluminium coordination polyhedron in UiO-15-125 differs significantly from the slightly distorted trigonal bipyramid in UiO-15-as. The AlO_5 -coordination polyhedron in UiO-15-125 can best be described as a distorted tetragonal pyramid having O5, O5' (OH groups), O3 and O4 in the basal plane and O2 in the apical position ($\text{O3}-\text{Al}-\text{O4}=156.0$ and $\text{O5}-\text{Al}-\text{O5}'=150.1^\circ$).

The infinite chains of aluminium polyhedra along [010] in UiO-15-as are maintained in UiO-15-125 as corner-sharing chains of tetragonal pyramids crosslinked by phosphate groups [Fig. 7(b)]. UiO-15-125 is described in terms of three-, four- and six-membered rings, just as for UiO-15-as above.

The hydrogen bonding in UiO-15-125 is quite similar to that in UiO-15-as (Table 9). The ethylenediammonium ions retain their parallel orientation to the inorganic layers and the previously described hydrogen bonding scheme. The only difference is that all the terminal phosphonyl oxygens of UiO-15-125 accept three hydrogen bonds from the nitrogen atoms of the ethylenediammonium ions.

The transformation of UiO-15-as into UiO-15-125 can be summarised as a dehydration process connected with small atomic displacements which perturbs the bonds and bond angles of the aluminium polyhedra and induces small changes in the hydrogen bonding scheme.

Crystal structure of UiO-15-225

The high temperature phase UiO-15-225, $[\text{NH}_3(\text{CH}_2)_2\text{-NH}_3]^{2+}[\text{Al}_2\text{O}(\text{PO}_4)_2]^{2-}$, is also a layered aluminophosphate

Table 9 Probable hydrogen bond lengths in UiO-15-125 and UiO-15-225

Hydrogen bond	Distance/Å (UiO-15-125)	Distance/Å (UiO-15-225)
N1...O1	2.77	2.79
N1...O1	2.76	2.90
N1...O1	2.96	2.78

Table 10 Bond valence analysis of UiO-15-225

	P	Al	$\Sigma=$
O1	1.50		1.50
O2	1.09	0.75	1.84
O3	1.20	0.76	1.96
O4	1.24	0.79	2.03
O5	0.92/1.84	1.84	
$\Sigma=$	5.03	3.22	

as shown in Fig. 6(c) and 7(c). The phase is formed when half of the bridging OH groups between the Al tetragonal pyramids of UiO-15-125 are removed from the structure by combining with hydrogen from the second OH so that a water molecule is released. Thus both the OH bridges are broken during the transformation. From the ring description point of view, this implies that the three- and six-membered rings of UiO-15-125 are converted into eight-membered rings. The transformation is however first completed after the formation of an Al–O–Al bond which closes each eight-membered ring resulting in the formation of two five-membered rings [Fig. 8(b)]. The transformation from UiO-15-125 to UiO-15-225 involves both bond breaking and bond formation and is of a topochemical nature.

The Al–O–Al bonds between Al-tetrahedra in UiO-15-225 are the first example of such bonding in an aluminophosphate. Just as for the aluminosilicate zeolites, all aluminophosphates discovered until now have obeyed Loewensteins rule⁴⁵ with the avoidance of tetrahedral Al–O–Al connectivity. Bridging OH groups between five- and six-coordinated aluminium have been observed in $\text{AlPO}_4\text{-15}$ ³⁹ and $\text{AlPO}_4\text{-21}$ for example.⁴⁶ In $\text{AlPO}_4\text{-14A}$ ⁴⁷ there are aluminium tetrahedra containing two OH bridges to neighbouring Al octahedra. But no direct Al–O–Al bond between tetrahedra has, to our knowledge, been observed previously for aluminophosphates.

UiO-15-225 has the same symmetry as UiO-15-125, and hence single crystallographic sites for aluminium and phosphorus. The phosphate tetrahedra are again coordinated with three bridging oxygens (O2, O3 and O4) to aluminium with an average bond distance of $d(\text{P}-\text{O})=1.557$ Å (Table 7). The fourth is a terminal phosphonyl oxygen at a distance of $d(\text{P}-\text{O1})=1.466$ Å. The aluminium tetrahedra also have three bridging oxygens to phosphorus at an average distance of $d(\text{Al}-\text{O})=1.749$ Å. The last oxygen bridge to Al is shorter $d(\text{Al}-\text{O5})=1.681$ Å. The hydrogen bonding scheme of UiO-15-225 is identical to that of UiO-15-125 (Table 9).

A bond-valence analysis³⁸ of UiO-15-225 (Table 10) indicates that the bridging O5 between the Al tetrahedra is only slightly underbonded. On the other hand the valence of the Al atom is a bit above the nominal value of +3. There seems to be a compromise between these effects in the crystal structure. In other structures containing directly linked AlO_4 tetrahedra, like the aluminate sodalites, e.g. $\text{Ca}_8(\text{AlO}_2)_{12}(\text{WO}_4)_2$,⁴⁸ and in the mineral bicchulite $\text{Ca}_8(\text{Al}_2\text{SiO}_6)_4(\text{WO}_4)_2$,^{49,50} the bridging O atoms are more clearly underbonded with respect to the contributions from Al alone, but their valence is fulfilled by means of coordination to the divalent cations. Such a stabilising effect is not present in UiO-15-225 where the ethylenediammonium ions are hydrogen bonded to the terminal O1 atoms only.

References

- 1 K. O. Kongshaug, H. Fjellvåg and K. P. Lillerud, *Microporous Mesoporous Mater.*, in press.
- 2 L. Vidal, V. Gramlich, J. Patarin and Z. Gabelica, *Eur. J. Solid State Inorg. Chem.*, 1998, **35**, 545.
- 3 R. H. Jones, J. M. Thomas, R. Xu, A. K. Cheetham and A. V. Powell, *J. Chem. Soc., Chem. Commun.*, 1991, 1266.
- 4 J. M. Thomas, R. H. Jones, R. Xu, J. Chen, A. M. Chippindale,

- S. Natarajan and A. K. Cheetham, *J. Chem. Soc., Chem. Commun.*, 1992, 929.
- 5 A. M. Chippindale, S. Natarajan, J. M. Thomas and R. H. Jones, *J. Solid State Chem.*, 1994, **111**, 18.
 - 6 K. Morgan, G. Gainsford and N. Milestone, *J. Chem. Soc., Chem. Commun.*, 1995, 425.
 - 7 P. A. Barrett and R. H. Jones, *J. Chem. Soc., Chem. Commun.*, 1995, 1979.
 - 8 D. A. Bruce, A. P. Wilkinson, M. G. White and J. A. Bertrand, *J. Chem. Soc., Chem. Commun.*, 1995, 2059.
 - 9 S. Oliver, A. Kuperman, A. Lough and G. A. Ozin, *Inorg. Chem.*, 1996, **35**, 6373.
 - 10 D. A. Bruce, A. P. Wilkinson, M. G. White and J. A. Bertrand, *J. Solid State Chem.*, 1996, **125**, 228.
 - 11 I. D. Williams, Q. Gao, J. Chen, L.-Y. Ngai, Z. Lin and R. Xu, *Chem. Commun.*, 1996, 1781.
 - 12 A. M. Chippindale, A. R. Cowley, Q. Huo, R. H. Jones, A. D. Law, J. M. Thomas and R. Xu, *J. Chem. Soc., Dalton Trans.*, 1997, 2639.
 - 13 Q. M. Gao, B. Z. Li, J. S. Chen, S. G. Li, R. Xu, I. D. Williams, J. Q. Zheng and D. Barber, *J. Solid State Chem.*, 1997, **129**, 39.
 - 14 J. Yu and I. D. Williams, *J. Solid State Chem.*, 1998, **136**, 141.
 - 15 N. Togashi, J. Yu, S. Zheng, K. Sugiyama, K. Hiraga, O. Terasaki, W. Yan, S. Qiu and R. Xu, *J. Mater. Chem.*, 1998, **8**, 2827.
 - 16 A. M. Chippindale, A. V. Powell, L. M. Bull, R. H. Jones, A. K. Cheetham, J. M. Thomas and R. Xu, *J. Solid State Chem.*, 1992, **96**, 199.
 - 17 S. Oliver, A. Kuperman, A. Lough and G. A. Ozin, *Chem. Commun.*, 1996, 1761.
 - 18 S. Oliver, A. Kuperman, A. Lough and G. A. Ozin, *Chem. Mater.*, 1996, **8**, 2391.
 - 19 J. Yu, K. Sugiyama, K. Hiraga, N. Togashi, O. Terasaki, Y. Tanaka, S. Nakata, S. Qiu and R. Xu, *Chem. Mater.*, 1998, **10**, 3636.
 - 20 K. Morgan, G. Gainsford and N. Milestone, *Chem. Commun.*, 1997, 61.
 - 21 M. A. Leech, A. R. Cowley, K. Prout and A. M. Chippindale, *Chem. Mater.*, 1998, **10**, 451.
 - 22 Z. Bircsak and W. T. A. Harrison, *Chem. Mater.*, 1998, **10**, 3016.
 - 23 J. W. Richardson, Jr., J. V. Smith and J. J. Pluth, *J. Phys. Chem.*, 1990, **94**, 3365.
 - 24 E. B. Keller, W. M. Meier and R. M. Kirchner, *Solid State Ionics*, 1990, **43**, 93.
 - 25 M. J. Annen, D. Young, M. E. Davis, O. B. Cavin and C. R. Hubbard, *J. Phys. Chem.*, 1991, **95**, 1380.
 - 26 S. Oliver, A. Kuperman and G. A. Ozin, *Angew. Chem. Int. Ed.*, 1998, **37**, 46.
 - 27 P. E. Werner, L. Eriksson and J. Westdahl, *J. Appl. Crystallogr.*, 1985, **18**, 367.
 - 28 J. Rodriguez-Caravajal, in *Collected Abstracts of Powder Diffraction Meeting*, Toulouse, France, 1990, p. 127.
 - 29 A. Le Bail, H. Duroy and J. Fourquet, *Mater. Res. Bull.*, 1988, **23**, 447.
 - 30 G. Cascarano, L. Favia and C. Giacobozzo, *J. Appl. Crystallogr.*, 1992, **25**, 267.
 - 31 Molecular Simulations Inc., San Diego, CA, 1997.
 - 32 A. Larson and R. B. von Dreele, GSAS, LANSCE, Copyright 1985–1988 by the Regents of the University of California.
 - 33 Biosym Technologies, San Diego, CA, 1995.
 - 34 C. Baerlocher, A. Hepp and W. M. Meier, DLS-76 a Program for the Simulation of Crystal Structures by Geometric Refinement, ETH, Zürich, 1977.
 - 35 A. Boulton and D. Louer, *J. Appl. Crystallogr.*, 1991, **24**, 987.
 - 36 A. Altomare, M. C. Burla, M. Camalli, B. Carrozzini, G. Cascarano, C. Giacobozzo, A. Guagliardi, A. G. G. Moliterni, G. Polidori and R. Rizzi, *Mater. Sci. Forum*, 1998, **278**, 284.
 - 37 A. Altomare, M. C. Burla, G. Cascarano, C. Giacobozzo, A. Guagliardi, A. G. G. Moliterni and G. Polidori, *J. Appl. Crystallogr.*, 1995, **28**, 842.
 - 38 I. D. Brown and D. Altermatt, *Acta Crystallogr., Sect. B*, 1985, **41**, 244.
 - 39 J. B. Parise, *Acta Crystallogr., Sect. C*, 1984, **40**, 1641.
 - 40 D. Riou, T. Loiseau and G. Férey, *J. Solid State Chem.*, 1993, **102**, 4.
 - 41 L. J. Sawers, V. J. Carter, A. R. Armstrong, P. G. Bruce, P. A. Wright and B. E. Gore, *J. Chem. Soc., Dalton Trans.*, 1996, 3159.
 - 42 H. Wozzala, T. Goetze, D. Fratzky and M. Meisel, *Acta Crystallogr., Sect. C*, 1998, **54**, 283.
 - 43 C. Panz, K. Polborn and P. Behrens, *Inorg. Chim. Acta*, 1998, **269**, 73.
 - 44 L. M. Meyer and R. C. Haushalter, *Chem. Mater.*, 1994, **6**, 349.
 - 45 W. Loewenstein, *Am. Mineral.*, 1954, **39**, 62.
 - 46 J. M. Bennett, J. P. Cohen, G. Artioli, J. J. Pluth and J. V. Smith, *Inorg. Chem.*, 1985, **24**, 188.
 - 47 J. J. Pluth and J. V. Smith, *Acta Crystallogr., Sect. C*, 1987, **43**, 866.
 - 48 W. Depmeier, *Acta Crystallogr., Sect. C*, 1984, **40**, 226.
 - 49 A. K. Gupta and A. D. Chatterjee, *Am. Mineral.*, 1978, **63**, 58.
 - 50 K. Sahl, *Z. Kristallogr.*, 1980, **152**, 13.